

## **SPECTRAL RADIATIVE HEAT TRANSFER ANALYSIS OF THE PLANAR SOFC**

**David L. Damm**

**Andrei G. Fedorov\***

Multiscale Integrated Thermofluidics Lab  
Woodruff School of Mechanical Engineering  
Georgia Institute of Technology  
Atlanta, Georgia 30332-0405

### **ABSTRACT**

Thermo-mechanical failure of components in planar-type solid oxide fuel cells (SOFCs) depends strongly on the local temperature gradients at the interfaces of different materials. Therefore, it is of paramount importance to accurately predict the temperature fields within the stack, especially near the interfaces. Because of elevated operating temperatures (of the order of 1000 K or even higher), radiation heat transfer could become a dominant mode of heat transfer in the SOFCs. In this study, we extend our recent work on radiative effects in solid oxide fuel cells (Journal of Power Sources, Vol. 124, No. 2, pp. 453-458) by accounting for the spectral dependence of the radiative properties of the electrolyte material. The measurements of spectral radiative properties of the polycrystalline yttria-stabilized zirconia (YSZ) electrolyte we performed indicate that an optically thin approximation can be used for treatment of radiative heat transfer. To this end, the Schuster-Schwartzchild two-flux approximation is used to solve the radiative transfer equation (RTE) for the spectral radiative heat flux, which is then integrated over the entire spectrum using an N-band approximation to obtain the total heat flux due to thermal radiation. The divergence of the total radiative heat flux is then incorporated as a heat sink into a 3-D thermo-fluid model of a SOFC through the user-defined function utility in the commercial FLUENT CFD software. The results of sample calculations are reported and compared against the baseline cases when no radiation effects are included and when the spectrally gray approximation is used for treatment of radiative heat transfer.

### **INTRODUCTION**

Accurate thermal modeling of the planar-type, anode-supported solid oxide fuel cell (SOFC), is a prerequisite to

understanding and predicting thermo-mechanical failure of cell components. Local temperature gradients at the interfaces of different components lead to mechanical stresses, which can in turn lead to the growth of cracks, delamination, and other defects which degrade the performance and efficiency of the cell.

Because of the elevated operating temperature (900-1100 K), it is expected that radiation heat transfer cannot simply be neglected, but should be given careful treatment in thermal modeling efforts. Within the unit cell of SOFCs, two major types of radiative heat transfer have been considered to some extent, albeit in a highly simplified and not always accurate fashion:

- within participating media such as porous or optically thin cell components, and participating gases found in the fuel and air channels [1, 2].
- surface radiation within the fuel and air channels, or from the cell to the environment [2-4].

Because the inclusion of radiation in overall CFD-electrochemical modeling of the cell can result in dramatic increases in computational cost [1, 4], identification and development of modeling methods that strike a balance between accuracy and computational efficiency has become a priority. Accomplishment of this goal will transform thermal modeling into a more effective design tool for the development of SOFCs by eliminating the need to make questionable assumptions about the role of radiative heat transfer for the sole purpose of reducing computational cost.

In our previous work [1] a framework for modeling radiation within the optically thick porous electrodes, and optically thin yttria-stabilized zirconia (YSZ) electrolyte, was developed. It was shown that the radiative effects are significant for thicker, semitransparent electrolytes, reducing

\* Corresponding Author 404-385-1356 (phone), 404-894-8496 (fax),  
[andrei.fedorov@me.gatech.edu](mailto:andrei.fedorov@me.gatech.edu) (email)

the overall operating temperature and decreasing thermal gradients in the monolith type cell. Also, it was shown that the Schuster-Schwarzchild's two-flux approximation gives accurate results at a fraction of the computational cost of the discrete ordinates (DO) method. In that work, however, knowledge of the relevant radiative properties was limited, and the models were developed assuming gray properties.

In this work, we report on experimental measurements of optical properties of the SOFC materials. Since the optical properties exhibit significant spectral variation, the radiative transfer model is formulated on a spectral basis, still in the optically thin limit of the two-flux approximation, and used to solve the radiative transfer equation (RTE) in the YSZ electrolyte layer. The N-band approximation is used for calculations of the total radiative heat flux. The divergence of the radiative heat flux is then incorporated into the overall energy conservation equation as a heat sink term through the user defined function utility in the FLUENT CFD model of the SOFC. The cell geometry under consideration is shown in Fig. 1., with relevant dimensions, properties, and operating conditions given in Table 1.

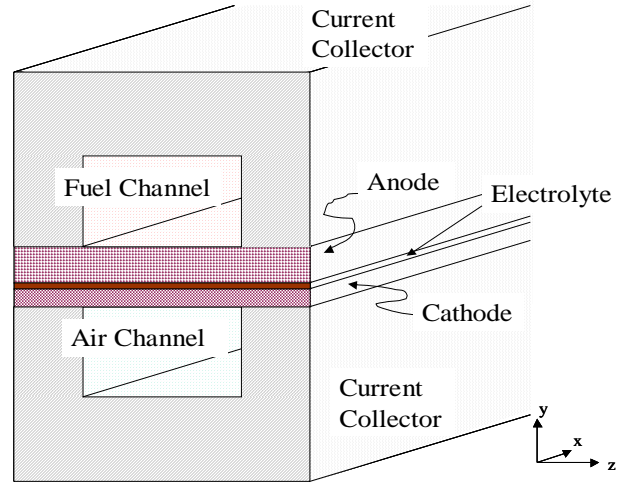


Figure 1. Schematic of the planar, anode-supported unit cell model of SOFC (not to scale).

## NOMENCLATURE

$E_{b\lambda}$	Blackbody emissive power [W/m <sup>2</sup> μm]
$k$	absorptive index of medium
$n$	refractive index of medium
$q_{\lambda}$	spectral radiative heat flux [W/m <sup>2</sup> μm]
$q_r$	total radiative heat flux [W/m <sup>2</sup> ]
$R$	reflectance of slab [%]
$Tr$	transmittance of slab [%]

### Greek Letters

$\beta$	extinction coefficient [1/m]
$\varepsilon$	emissivity of boundary
$\kappa$	absorption coefficient [1/m]
$\lambda$	wavelength [μm]
$\rho$	reflectivity
$\sigma$	Stefan-Boltzmann constant [J/K <sup>4</sup> m <sup>2</sup> s]
$\sigma_s$	scattering coefficient of medium
$\tau$	transmittivity
$\tau_{\lambda}$	spectral optical thickness
$\omega$	single scattering albedo
$\Psi$	non-dimensional radiative heat flux

## 1. Measurement of Radiative Properties

Accounting for radiative heat transfer within solid semitransparent materials requires knowledge of the radiative properties, namely absorption coefficient,  $\kappa$ , and refractive index,  $n$ . Radiative properties typically vary with wavelength, and we used Planck's law [5] to find the relevant spectral range for measurements. For typical operating temperatures of 900–1100 K and  $n = 1.8$  [1], it can be shown that over 90% of the emissive power is contained within the near to mid infrared spectral region,  $0.9 < \lambda < 7.8$  μm. Figure 2 shows the emissive power as a function of wavelength for these conditions.

A Fourier transform infrared (FTIR) spectrometer (Bruker Optics TENSOR 37) fitted with a reflectance accessory was used to obtain transmittance,  $Tr$ , and reflectance,  $R$ , data for samples of YSZ, nickel-doped YSZ, and strontium-doped

Lanthanum ferrite (LSF)—materials commonly used for the electrolyte, anode, and cathode, respectively, of SOFCs. For collecting near-IR data, an InGaAs detector and quartz beam splitter were used, and for the mid-IR data, a KBr/DLaTGS collector and Ge on KBr substrate beam splitter were used. All measurements were performed at room temperature. For 200 μm thick samples of Ni-YSZ, and LSF, the transmittance was essentially zero within the noise of the measurements. Thus, we assumed that the electrodes are opaque in this region of the spectrum, although scattering could play a role in radiative transfer and should be investigated further. The 330 μm thick sample of polycrystalline YSZ, however, is semitransparent and shows significant spectral variation in transmittance and reflectance as seen in Fig. 3.

This transmittance and reflectance data can be related to the transmittivity,  $\tau$ , and reflectivity,  $\rho$ , through geometric optics and ray tracing methods [5] via simultaneous solution of the following equations:

$$R = \rho \left[ 1 + \frac{(1-\rho)^2 \tau^2}{1-\rho^2 \tau^2} \right] \quad (1.1)$$

and,

$$Tr = \frac{(1-\rho)^2 \tau}{1-\rho^2 \tau^2} \quad (1.2)$$

Once transmittivity and reflectivity are calculated, the absorptive index,  $k$ , is found from,

$$k = -\frac{n\lambda \ln[\tau]}{4\pi d} \quad (1.3)$$

where,  $d$  is the thickness of the sample. The refractive index,  $n$ , can be approximately found using Fresnel's equation [5] by assuming that the material of interest has low absorptive index,

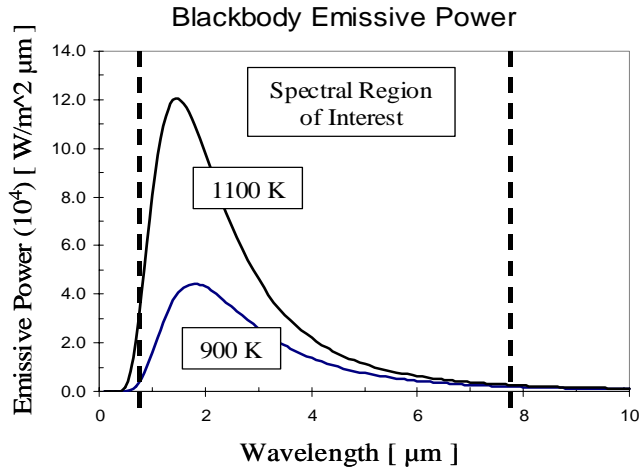


Figure 2. Definition of the spectral range of interest wherein 90% of radiative energy falls according to Planck's law for blackbody emissive power ( $n=1.8$ ) for the temperatures relevant to SOFCs.

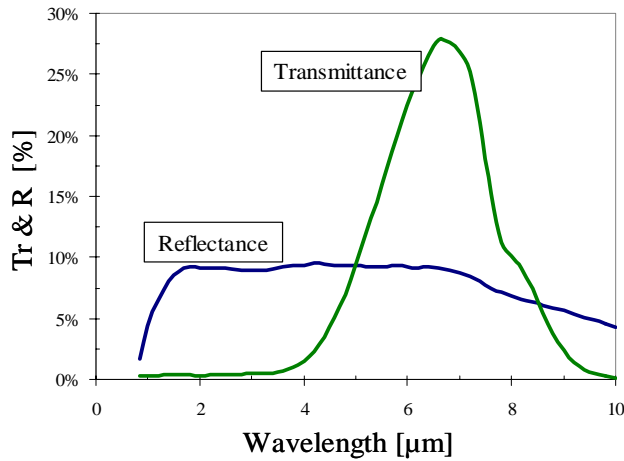


Figure 3. FTIR transmittance and reflectance data for a 330  $\mu\text{m}$  thick sample of polycrystalline yttria-stabilized zirconia (YSZ).

$$\rho = \frac{(1-n)^2 + k^2}{(1+n)^2 + k^2} \quad (1.4)$$

Finally, the spectral absorption coefficient,  $\kappa$ , is related to the absorptive index by,

$$\kappa = \frac{4\pi k}{n\lambda} \quad (1.5)$$

where,  $\lambda$  is the wavelength of the radiation. The resulting absorption coefficient, found by processing FTIR data using the method described above, is plotted in Fig. 4. For a typical electrolyte thickness of 15 $\mu\text{m}$ , the resulting spectral optical thickness,  $\tau_\lambda$ , of the electrolyte layer varies between 0.07 and 0.24 in the spectral region of interest. Thus, a spectral, optically thin approximation is appropriate for solving the radiative transfer equation in the electrolyte [5].

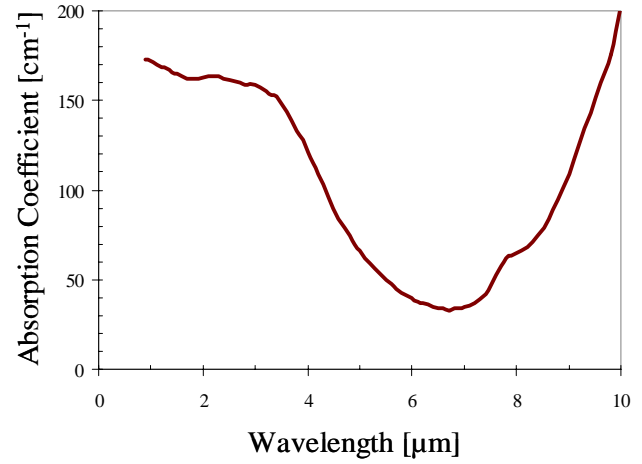


Figure 4. Absorption coefficient of YSZ computed from transmittance and reflectance measurements showing strong spectral dependence.

## 2. Formulation of Two-Flux Model

The formulation of radiation heat transfer analysis for the optically thin YSZ electrolyte begins with writing the radiative transfer equation (RTE) [5] for a participating medium, and applying it to a 1-D plane-parallel medium. The Schuster and Schwartzschild's, or two-flux, approximation assumes that the radiative intensity is uniform over the upper and lower hemispheres. Also, assuming isotropic scattering in the YSZ, the RTE can be rewritten as an ODE for the spectral heat flux [5],

$$\frac{d^2 q_\lambda}{d\tau_\lambda^2} - (1-\omega_\lambda)(4q_\lambda) = (1-\omega_\lambda)4 \frac{dE_{b\lambda}}{d\tau_\lambda} \quad (2.1)$$

where,  $q_\lambda$  is the spectral radiative heat flux,  $\tau_\lambda = \int_0^s \beta_\lambda ds$  is the

spectral optical thickness for extinction,  $\omega_\lambda = \frac{\sigma_{s\lambda}}{\beta_\lambda}$  is the single

scattering albedo, and  $E_{b\lambda}$  is the spectral, black-body emissive power. The boundary conditions for diffuse surfaces can be expressed, after some manipulation, as,

$$\begin{aligned} \tau_\lambda = 0: & \quad -\frac{(1-\rho_1)}{1-\omega} \frac{dq_\lambda}{d\tau_\lambda} + 2(1+\rho_1)q_\lambda = 4(\varepsilon E_{b\lambda})_1 - (1-\rho_1)4E_{b\lambda} \\ \tau_\lambda = \tau_{\lambda,L}: & \quad -\frac{(1-\rho_2)}{1-\omega} \frac{dq_\lambda}{d\tau_\lambda} - 2(1-\rho_2)q_\lambda = 4(\varepsilon E_{b\lambda})_2 - (1-\rho_2)4E_{b\lambda} \end{aligned} \quad (2.2)$$

where,  $\rho$  is the reflectivity of the boundaries, (subscripts 1 and 2 indicate properties at the boundaries),  $\varepsilon$  is the emissivity of the boundaries, and  $\tau_{\lambda,L}$  is the spectral optical thickness of the 1-D layer. Equation (2.1) was solved for spectral radiative heat flux as a function of spectral optical thickness, however, the solution obtained is only semi-analytical, containing integrals

Table 1. SOFC Unit Cell Dimensions, Material Properties, and Operating Conditions

Region	Type	Size/Thickness	Density [kg/ m <sup>3</sup> ]	Thermal Conductivity [W/m K]
Cathode	Porous (0.3)	75 μm	3030	5.84
Anode	Porous (0.4)	500 μm	3310	1.86
Electrolyte	Solid	15 μm	5160	2.16
Current collector	Solid	5 mm	8030	20.0
Cell Length (x-direction)		10 cm		
Cell Width (z-direction)		5 mm		
Air/Fuel Channels		2.5 x 3.0 mm		
Fuel Inlet (1000 K)	80% H <sub>2</sub>	20% H <sub>2</sub> O		85% utilization
Air Inlet (1000 K)	21% O <sub>2</sub>	79% N <sub>2</sub>		20% utilization

of the blackbody emissive power that were numerically approximated.

Once the spectral radiative heat flux is determined, total radiative heat flux is obtained by integration of the spectral heat flux over the entire electromagnetic spectrum,

$$q_r = \int_0^{\infty} q_\lambda d\lambda \quad (2.3)$$

Numerically, the spectral integration is accomplished through the N-band approximation method [5,6], which assumes that spectral properties, (in this case the extinction coefficient), are approximately constant over discrete wavelength intervals and replaces the integral by a summation.

### 3. Model Validation

In order to validate the semi-analytical solution we developed for solving the spectral RTE (Eq. 2.1) for the optically-thin electrolyte, the numerical solution was compared to an analytical solution given by Modest [5] for an isothermal problem as well as to a simple 1-D combined conduction-radiation problem solved using FLUENT's built in Discrete Ordinates (DO) method.

The radiative heat flux in a gray, isothermal, non-scattering, 1-D, plane-parallel medium between two black walls at equal temperatures (Fig 6.), is given by the following approximation [5],

$$q = n^2 \sigma (T^4 - T_w^4) \left[ e^{-2(\tau_L - \tau)} - e^{-2\tau} \right] \quad (3.1)$$

where,  $\sigma$  is the Stefan-Boltzmann constant,  $T$  and  $T_w$  are the absolute temperatures of the medium and walls, respectively, and  $\tau$  is the optical length. A dimensionless heat flux is then defined [5] as:

$$\Psi = \frac{q}{n^2 \sigma (T^4 - T_w^4)} = e^{-2(\tau_L - \tau)} - e^{-2\tau} \quad (3.2)$$

Figure 5 compares numerical predictions of the wall heat flux obtained using our spectral algorithm (but using gray properties) and an approximate solution given by Eq. (3.2). In

the simulations, the temperatures of the walls and medium are taken to be 1000K and 900K, respectively. Clearly, the results

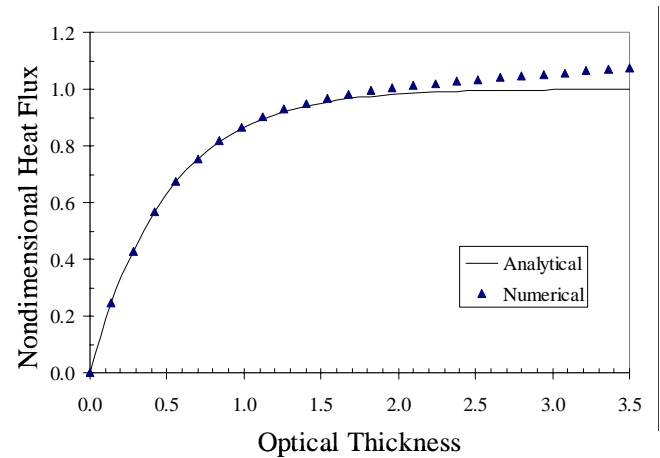


Figure 5. Comparison of the numerical predictions obtained using the spectral two-flux model with the analytical solution (eqn. 3.2) for the non-dimensional wall heat flux.

agree very well for optical thickness up to approximately 2.0.

Further validation of the solution algorithm demands comparison of the results for the problem involving both radiation and conduction. To this end, the spectral two-flux model was implemented in FLUENT CFD software as a user defined function, which incorporates the divergence of the radiative heat flux as a heat sink in the energy equation. In order to validate this implementation, a simple problem was considered of combined radiative-conductive heat transfer in a 1-D, plane-parallel medium bounded by two isothermal plates (Fig. 6.). The temperatures of the upper plate and lower plate were fixed at 1200 K and 800 K, respectively. The temperature field within the medium was solved using the discrete ordinate (DO) method (standard FLUENT implementation) as well as by using the user-defined utility for the two-flux approximation that we developed. A comparison of the results for optical thickness of 0.001, 0.1, and 1.0 shown in Fig. 7 clearly indicates the robustness of the developed spectral two-flux radiation modeling algorithm.

In addition to testing the two-flux model implementation on these gray problems, a spectral case was also considered by using three spectral bands to approximate the spectral

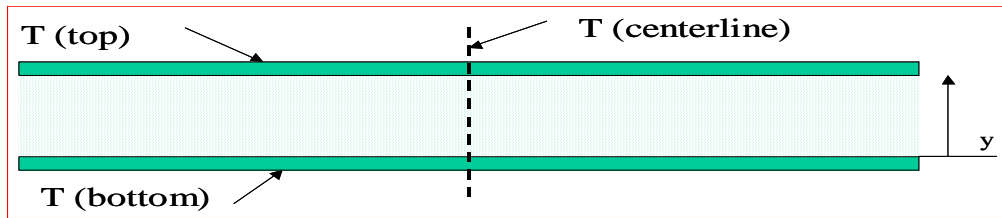


Figure 6. A simple problem of radiation-conduction heat transfer in a 1-D, plane-parallel medium bounded between two isothermal plates used for validation of the spectral two-flux radiation model.

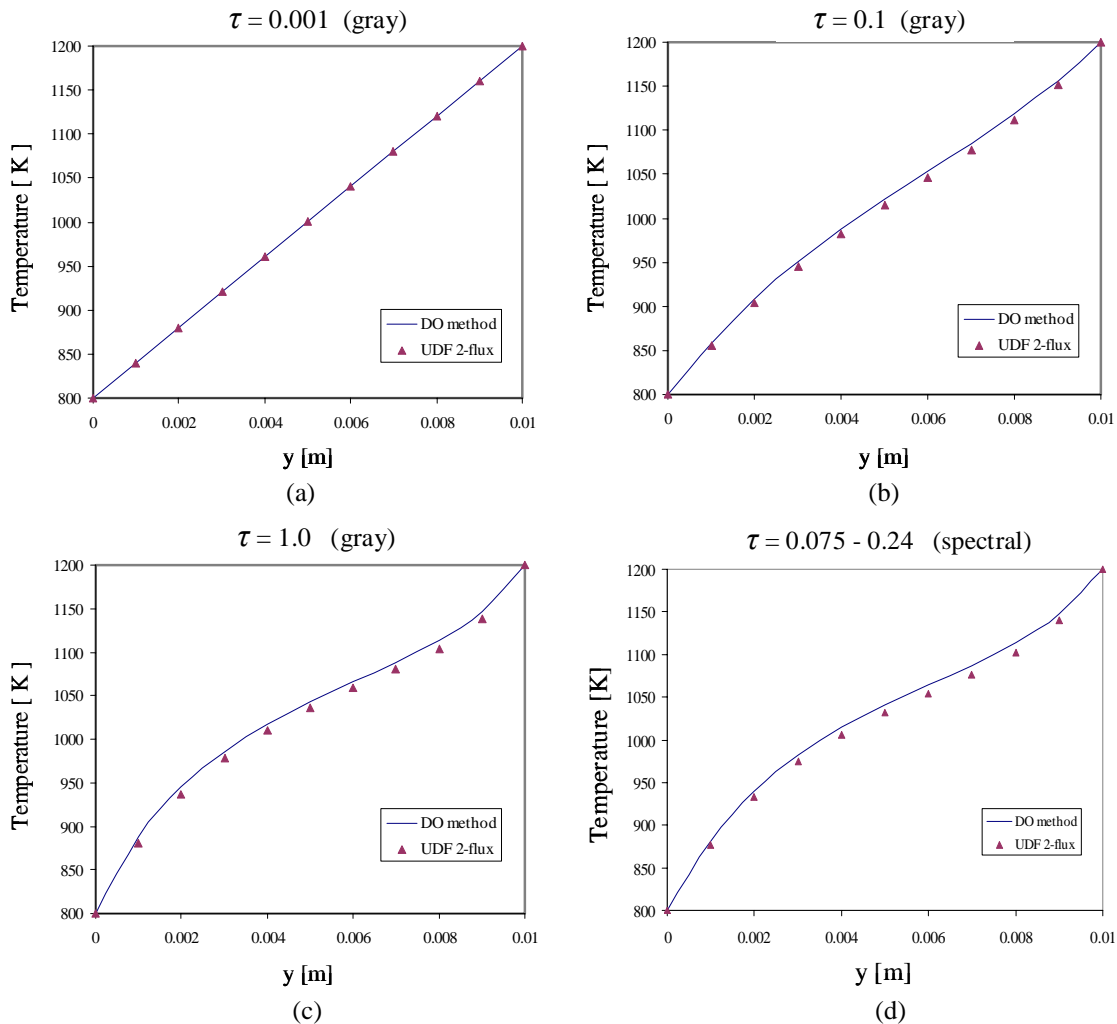


Figure 7. Comparison of results obtained using the two-flux and discrete ordinates (benchmark) methods for various optical thicknesses and gray optical properties (a-c), and spectrally varying absorption coefficient (d).

dependence of the extinction (absorption) coefficient of the electrolyte (obtained from measurement results in Fig. 4),

$$\beta = \begin{cases} 160 \text{ cm}^{-1}; & 0.0 < \lambda < 3.5 \\ 110 \text{ cm}^{-1}; & 3.5 \leq \lambda < 5.0 \\ 50 \text{ cm}^{-1}; & 5.0 \leq \lambda < \infty \end{cases} \quad (3.3)$$

These values correspond to optical thicknesses of 0.24, 0.165, and 0.075 for three respective spectral bands in the case of a

15 $\mu\text{m}$  thick electrolyte. Figure 7 shows a comparison between the temperature predictions obtained using the two-flux model and FLUENT's standard discrete ordinate method for the 3-band spectral model. In this simulation, the boundaries were assumed gray ( $\epsilon = 0.9$ ), with an isotropically scattering medium ( $\omega = 0.1$ ). Once again, the agreement appears to be satisfactory. Although the medium is assumed to be isotropically scattering, the single scattering albedo is not known, and for the remainder of this work, was assumed zero.

#### 4. Spectral Radiative Analysis of SOFC Unit Cell

Solution of the momentum, energy, and species conservation equations that describe species transport and the temperature field in the unit cell of an SOFC stack was obtained using FLUENT CFD software as described in our previous work [1]. The electrochemical reactions and the potential field within the cell were solved by an add-on tool developed by the Department of Energy's National Energy Technology Laboratory, which is described in [7, 8]. The unit cell geometry, materials properties, and the standard operating conditions under consideration are given in Table 1. The FLUENT model of SOFC unit cell was discretized using a fine mesh of 105,600 elements. The appropriateness of this mesh was verified against another model of 262,500 elements, and the results from both models compared favorably. Because the unit cell is part of a larger stack, the boundaries were considered adiabatic. The electrodes were modeled as porous media, and the electrolyte as a solid region. In this model, the current density of the cell was specified ( $150 \text{ mA/cm}^2$ ), resulting in an average operating voltage of 0.87 V and average cell temperature of 1046 K.

Because the temperature gradients at interfaces are of particular interest for thermomechanical failure analysis, Fig. 8 shows a comparison of the temperature distribution at the anode-electrolyte and cathode-electrolyte interfaces for the cases with and without radiation in the electrolyte layer. Clearly, the effect of radiation is minimal, leading to at most a couple of degrees reduction in the interfacial temperature. This is in sharp contrast to our previous findings [1], wherein we reported significant reduction in temperature when radiation is included. This significant difference in results owes to difference in the cell geometry that was simulated in [1] and here. Specifically, a thick,  $500 \mu\text{m}$  electrolyte layer, leading to significant (relative to thermal radiation) conduction resistance, was simulated, whereas a more realistic electrolyte layer found in presently developed SOFC [8-10], which is only  $15 \mu\text{m}$  (or less) thick, was used in performing analysis reported in this paper. Thus, the conduction resistance across the electrolyte is reduced by a factor of more than 30, while the radiation resistance (optical thickness) remains approximately the same for both cases. The net result is domination of conduction heat transfer over radiative heat transfer even for such high operating temperatures as found in SOFCs.

In SOFCs, heat generated, due to the electrochemical reaction at the electrode-electrolyte interfaces and by ohmic heating in the electrolyte, is carried away mostly by flow in the air channel. Thus, the electrolyte acts as a thermal resistance to removing heat generated at the interface of the anode and electrolyte. It can be shown that for the geometry and operating conditions reported in [1], radiative heat transfer contributes approximately 15% to the total heat flux across the electrolyte in the presence of only 1 Kelvin temperature difference across the electrolyte at temperatures relevant to SOFCs. This is not the case for a very thin electrolyte, which must sustain much greater temperature gradients before radiation becomes significant.

Finally, although our results indicate that radiation within the electrolyte has little effect for the geometry and operating conditions used in this study, it cannot, in general, simply be neglected. For example, during the start-up and shut-down of the SOFC, one could develop significant temperature gradients

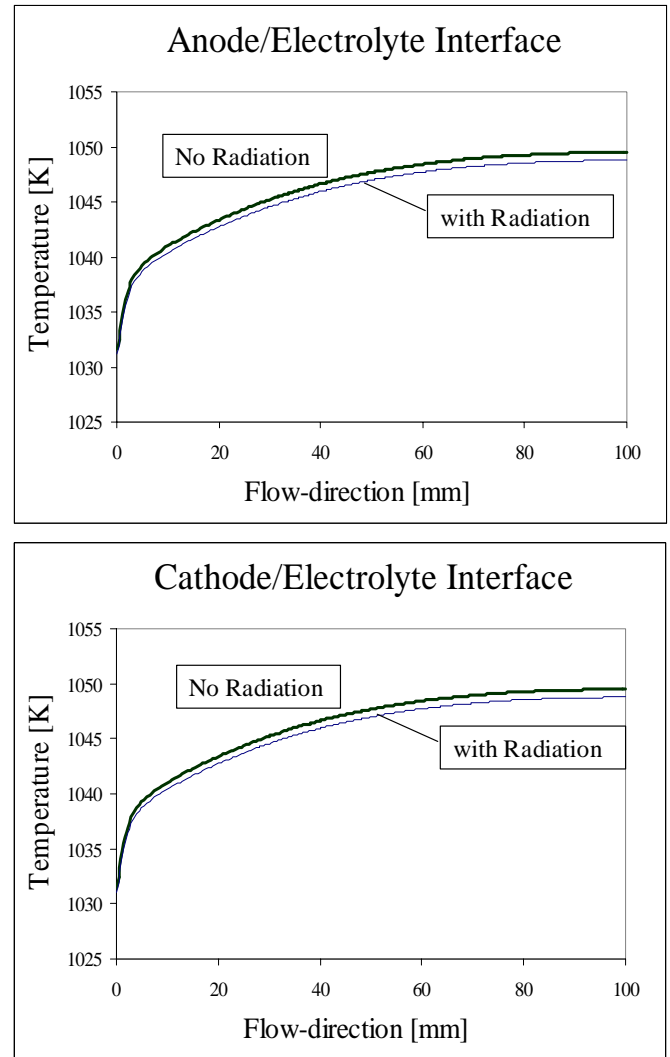


Figure 9. Temperature profile of the anode/electrolyte and cathode/electrolyte interfaces with and without radiation.

across even very thin electrolyte leading to potentially significant radiation effects. The major concern on whether or not to include the radiation analysis into the SOFC thermal model lies in the tremendous increase in computational costs associated with inclusion of radiation. This demands development of computationally efficient techniques for treatment of radiative heat transfer.

The spectral two-flux model we developed is sufficiently accurate and adds only 20% to the CPU time required to obtain the converged solution of the overall SOFC thermal-fluid model. This is in comparison to the approximately ten-fold increase in the CPU time required for computations if radiation is solved using the standard discrete ordinate (DO) method implemented in FLUENT. Thus, we would argue that the spectral two-flux treatment of radiative heat transfer is sufficiently accurate and computationally efficient to be included in any SOFC thermal-fluid analysis tool to study, on a case-by-case basis, variations in geometry, operating conditions, or electrolyte materials that could potentially induce significant temperature gradients across the electrolyte layer.

## 5. Conclusions and Future Work

In this paper, we report measurements and analysis of spectral radiative heat transfer as relevant to solid oxide fuel cells (SOFC). Specifically, the absorption coefficient and refractive index of the yttria-stabilized zirconia electrolyte (YSZ) were experimentally determined. It was found that the YSZ is optically thin for the electrolyte layer thicknesses relevant to currently developed SOFC, and optical properties exhibit strong wavelength dependence. The Schuster-Schwartzchild two-flux approximation was used to solve the RTE on a spectral basis with three spectral bands used to approximate spectral variation of the absorption coefficient. The model implementation was validated against an analytical solution from the literature for an isothermal case, as well as using the benchmark solution for one-dimensional conduction-radiation heat transfer across gray and non-gray layers obtained using the discrete ordinate method implemented in the FLUENT CFD software.

It was found that for the geometry, materials, and operating conditions used in this study, which are thought as being representative of SOFC systems currently under development, radiative heat transfer within the electrolyte has negligible effect on the average cell operating temperature, voltage, or temperature gradients at the interfaces of the electrolyte and electrodes. In general, however, the geometry, materials, and operating conditions of SOFCs that will eventually be brought to market are unknown at this time. And because the spectral two-flux model is demonstrated to be an accurate and computationally-efficient method of accounting for radiative heat transfer within optically thin layers, it can and should be used as a part of any sound thermal-fluid analysis of SOFC systems.

Our future work will focus on analyzing the effect of radiative heat transfer in transient (start-up or shut-down) situations, which potentially feature much larger thermal gradients across the electrolyte layer, and also on development of computationally-efficient models for calculating surface-to-surface radiation exchange within the air and fuel flow channels of SOFCs.

## ACKNOWLEDGMENTS

The support of this work by DOE through the Phase II SECA Program is acknowledged and appreciated.

## REFERENCES

[1] Murthy, S. and Fedorov, A. G., 2003, "Radiation Heat Transfer Analysis of the Monolith-Type Solid Oxide Fuel Cell", *Journal of Power Sources*, Vol. 124, No. 2, pp. 453-458.

[2] VanderSteen, J.D.J., Pharoah, J.G., 2004, "The Role of Radiative Heat Transfer with Participating Gases on the Temperature Distribution in Solid Oxide Fuel Cells", *Fuel Cell Science, Engineering and Technology*, Conf. Proceedings, ASME.

[3] Burt, A.C., Celik, I.B., Gemmen, R.S., Smirnov, A.V., 2003, "Influence of Radiative Heat Transfer on Variation of Cell Voltage Within a Stack", *Fuel Cell Science, Engineering and Technology*, Conf. Proceedings, ASME, pp. 217-223.

[4] Yakabe, H., Ogiwara, T., Hishinuma, M., Yasuda, I., 2001, "3-D Model Calculation for Planar SOFC", *Journal of Power Sources*, Vol. 102, pp. 144-154.

[5] Modest, M., *Radiative Heat Transfer*, 1<sup>st</sup> Edition, McGraw-Hill, 1993.

[6] Varady, M. and Fedorov, A. G., 2002, "Combined Radiation and Conduction in Glass Foams", *ASME Journal of Heat Transfer*, Vol. 124, No. 6, pp. 1103-1110.

[7] Prinkey, M.T., Gemmen, R.S., Rogers, W.A., 2001, "Application of a New CFD Analysis Tool for SOFC Technology", Proceedings of ASME IMECE 2001. HTD-Vol.369-4, pp. 291-300

[8] Rogers, W.A., Gemmen, R.S., Johnson, C., Prinkey, M., Shahnam, M., 2003, "Validation and Application of a CFD-based Model for Solid Oxide Fuel Cells and Stacks", *Fuel Cell Science, Engineering and Technology*, Conf. Proceedings, ASME, pp. 517-520.

[9] Autissier, N., Larrain, D., Van herle, J., Favrat, D., 2004, "CFD Simulation Tool for Solid Oxide Fuel Cells", *Journal of Power Sources*, Vol. 131, pp. 313-319.

[10] Khaleel, M.A., Lin, Z., Singh, P., Surdoval, W., Collin, D., 2004, A Finite Element Analysis Modeling Tool for Solid Oxide Fuel Cell Development: Coupled Electrochemistry, Thermal and Flow Analysis in MARC<sup>®</sup>, *Journal of Power Sources*, Vol. 130, pp. 136-148.